

Article

Toxic Kidney Damage in Rats Following Subchronic Intraperitoneal Exposure to Element Oxide Nanoparticles

Yuliya V. Ryabova ¹, Ilzira A. Minigalieva ¹, Marina P. Sutunkova ¹, Svetlana V. Klinova ^{1,*},
Alexandra K. Tsaplina ¹, Irene E. Valamina ², Ekaterina M. Petrunina ¹, Aristides M. Tsatsakis ^{3,4,*},
Charalampos Mamoulakis ⁵, Kostas Stylianou ⁶, Sergey V. Kuzmin ⁷, Larisa I. Privalova ¹
and Boris A. Katsnelson ¹

- ¹ Yekaterinburg Medical Research Center for Prophylaxis and Health Protection in Industrial Workers, 620014 Yekaterinburg, Russia
 - ² Department of Pathology, Ural State Medical University, 620028 Yekaterinburg, Russia
 - ³ Department of Forensic Sciences and Toxicology, Faculty of Medicine, University of Crete, 71003 Heraklion, Greece
 - ⁴ Department of Human Ecology and Environmental Hygiene, IM Sechenov First Moscow State Medical University, 119991 Moscow, Russia
 - ⁵ Department of Urology, University General Hospital of Heraklion, Medical School, University of Crete, 71003 Heraklion, Greece
 - ⁶ Department of Nephrology, University General Hospital of Heraklion, Medical School, University of Crete, 71003 Heraklion, Greece
 - ⁷ Federal Budgetary Establishment of Science “F.F. Erisman Scientific Centre of Hygiene” of the Federal Service for Surveillance on Consumer Rights Protection and Human Wellbeing, 141014 Mytishchi, Russia
- * Correspondence: klinova.svetlana@gmail.com (S.V.K.); aristsatsakis@gmail.com (A.M.T.)



Citation: Ryabova, Y.V.; Minigalieva, I.A.; Sutunkova, M.P.; Klinova, S.V.; Tsaplina, A.K.; Valamina, I.E.; Petrunina, E.M.; Tsatsakis, A.M.; Mamoulakis, C.; Stylianou, K.; et al. Toxic Kidney Damage in Rats Following Subchronic Intraperitoneal Exposure to Element Oxide Nanoparticles. *Toxics* **2023**, *11*, 791. <https://doi.org/10.3390/toxics11090791>

Academic Editors: Pamela Lein and Soisungwan Satarug

Received: 25 July 2023

Revised: 31 August 2023

Accepted: 12 September 2023

Published: 19 September 2023



Copyright: © 2023 by the authors. Licensee MDPI, Basel, Switzerland. This article is an open access article distributed under the terms and conditions of the Creative Commons Attribution (CC BY) license (<https://creativecommons.org/licenses/by/4.0/>).

Abstract: Chronic diseases of the urogenital tract, such as bladder cancer, prostate cancer, reproductive disorders, and nephropathies, can develop under the effects of chemical hazards in the working environment. In this respect, nanosized particles generated as by-products in many industrial processes seem to be particularly dangerous to organs such as the testes and the kidneys. Nephrotoxicity of element oxide particles has been studied in animal experiments with repeated intraperitoneal injections of Al₂O₃, TiO₂, SiO₂, PbO, CdO, CuO, and SeO nanoparticles (NPs) in total doses ranging from 4.5 to 45 mg/kg body weight of rats. NPs were synthesized by laser ablation. After cessation of exposure, we measured kidney weight and analyzed selected biochemical parameters in blood and urine, characterizing the state of the excretory system. We also examined histological sections of kidneys and estimated proportions of different cells in imprint smears of this organ. All element oxide NPs under investigation demonstrated a nephrotoxic effect following subchronic exposure. Following the exposure to SeO and SiO₂ NPs, we observed a decrease in serum creatinine and urea, respectively. Exposure to Al₂O₃ NPs caused an increase in urinary creatinine and urea, while changes in total protein were controversial, as it increased under the effect of Al₂O₃ NPs and was reduced after exposure to CuO NPs. Histomorphological changes in kidneys are associated with desquamation of the epithelium (following the exposure to all NPs except those of Al₂O₃ and SiO₂) and loss of the brush border (following the exposure to all NPs, except those of Al₂O₃, TiO₂, and SiO₂). The cytomorphological evaluation showed greater destruction of proximal sections of renal tubules. Compared to the controls, we observed statistically significant alterations in 42.1% (8 of 19) of parameters following the exposure to PbO, CuO, and SeO NPs in 21.1% (4 of 19)—following that, to CdO and Al₂O₃ NPs—and in 15.8% (3 of 19) and 10.5% (2 of 19) of indicators, following the exposure to TiO₂ and SiO₂ nanoparticles, respectively. Histomorphological changes in kidneys are associated with desquamation of epithelium and loss of the brush border. The cytomorphological evaluation showed greater destruction of proximal sections of renal tubules. The severity of cyto- and histological structural changes in kidneys depends on the chemical nature of NPs. These alterations are not always consistent with biochemical ones, thus impeding early clinical diagnosis of renal damage. Unambiguous ranking of the NPs examined by the degree of their nephrotoxicity is difficult. Additional studies are necessary to establish key indicators of the nephrotoxic effect, which can facilitate early diagnosis of occupational and nonoccupational nephropathies.

Keywords: kidney diseases; nanoparticles; nephrotoxicity; occupational exposure; oxides; urogenital system

1. Introduction

Kidney disease is widespread throughout the world. Nephropathies often have a long asymptomatic latency period because kidneys have enormous compensatory capabilities and can maintain homeostasis for years. Chronic kidney disease has been estimated to affect 9% to 15% of the population in different regions of the world [1]. It has a major effect on global health, both as a direct cause of global morbidity and mortality and as an important risk factor for cardiovascular disease, but it is largely preventable and treatable and deserves greater attention in global health-policy decision making, particularly in locations with low and middle sociodemographic indexes [2,3]. Chronic diseases of the urogenital tract, including bladder cancer, prostate cancer, reproductive disorders, and nephropathies, can be induced by exposure to hazardous chemicals at work [4–12]. Kidneys are particularly susceptible to the adverse effects of chemical pollutants. This organ filters almost 200 L of blood per day, producing up to 2 L of urine. As a result, pollutants have a strong impact on kidneys [13]. In their recent review, Lentini et al. [14] revealed correlations between acute and chronic kidney disease and environmental levels of heavy metals and other risk factors. The main components of the aerosol polluting the workplace air in the production of aluminum titanium alloys are Al, Ti, and Si [15]. Occupational exposure to selenium, copper, and their compounds occurs in metallurgy during copper sludge processing; roasting of copper pyrites; and manganese, selenium, and tellurium production [16,17]. The sources of environmental pollution with lead and cadmium, in addition to the mining and metallurgical industries, are the production of batteries and electroplating, urban road dust, cigarette smoke, etc. [18,19]. Besides this, workplace air pollution with metal oxide submicron and nanosized compounds generated as by-products is common for many industries. Understanding the mechanisms of nephrotoxicity of nanoparticles (NPs) can serve as a tool for the early diagnosis of occupational nephropathies, enabling timely treatment and a longer work ability of humans. The current scientific literature presents experimental studies on the damaging effect of NPs on the structure and function of the testes and kidneys following exposure through different routes [20–29].

The general and specific toxic effects of Al_2O_3 , TiO_2 , SiO_2 , PbO , and CdO NPs, as well as cytotoxic effects of CuO and SeO NPs, were discussed in detail in our previous works [15,30–33]. We have noted that Al_2O_3 , TiO_2 , SiO_2 , PbO , and CdO NPs exhibit multiple organ toxicity, including certain signs of kidney damage, on which we want to focus in this paper. The aim of the present study was to analyze nephrotoxic effects of subchronic exposures to NPs based on weight, biochemical, histomorphometric, and cytological indicators.

2. Materials and Methods

Suspensions of the element oxide (EO) nanoparticles (NPs) were prepared at the Center for Collective Use “Modern Nanotechnologies” of the Ural Federal University, Yekaterinburg, using laser ablation of thin-sheet targets of the corresponding material of 99.99% purity in sterile deionized water. The technique has been described in more detail elsewhere [13,14]. The stability of suspensions was characterized by their zeta potential, measured using the Zetasizer Nano ZS analyzer (Malvern Panalytical Ltd., Malvern, UK), and was found to be high (up to 42 mV), thus enabling an increase in particle concentrations up to 0.5 g/L by partial evaporation of water at 50 °C, without changing the size and chemical characteristics of EO NPs. The particle shape and size were characterized using scanning electron microscopy (SEM) and particle size distribution curves (d) (Table 1).

Experimental studies were conducted on outbred male albino rats aged 3 to 4 months at the beginning of the experiment. The weight variations of animals did not exceed

±20% of the mean weight of all the animals at the commencement of the studies. Repeated intraperitoneal injections thrice per week for six weeks (18 injections in total) were used to simulate subchronic toxicity. The animals were kept, fed, cared for, and removed from the experiment in strict accordance with the International Guiding Principles for Biomedical Research Involving Animals developed by CIOMS and ICLAS (2012). The animal study protocols were approved by the Institutional Ethics Committee of the Yekaterinburg Medical Research Center for Prophylaxis and Health Protection in Industrial Workers (Table 2). The choice of single doses of NPs under study was limited by the maximum concentration of stable NP suspensions and by the individual tolerance of animals established in previous pilot experiments. The exposure doses selected for the experiments induced moderate toxicity without causing pain to or the death of the animals. Experimental studies were conducted on outbred male albino rats aged 3 to 4 months at the beginning of the experiment. The weight variations of animals did not exceed ±20% of the mean weight of all the animals at the commencement of the studies. Repeated intraperitoneal injections thrice per week for six weeks (18 injections in total) were used to simulate subchronic toxicity. The animals were kept, fed, cared for, and removed from the experiment in strict accordance with the International Guiding Principles for Biomedical Research Involving Animals developed by CIOMS and ICLAS (2012). The animal study protocols were approved by the Institutional Ethics Committee of the Yekaterinburg Medical Research Center for Prophylaxis and Health Protection in Industrial Workers (Table 2). The choice of single doses of NPs under study was limited by the maximum concentration of stable NP suspensions and by the individual tolerance of animals established in previous pilot experiments. The exposure doses selected for the experiments induced moderate toxicity without causing pain to or the death of the animals.

Before euthanasia, 24-h urine specimens were collected to measure the urinary pH, protein, levels of urea, uric acid, and creatinine and to calculate endogenous creatinine clearance.

Table 1. Description of the nanoparticles used in animal experiments.

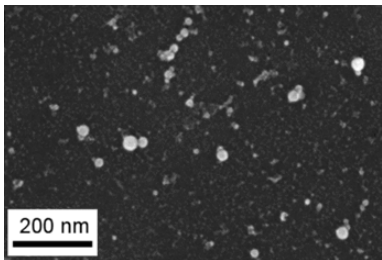
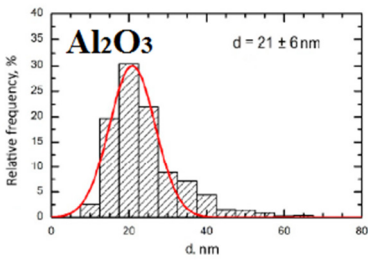
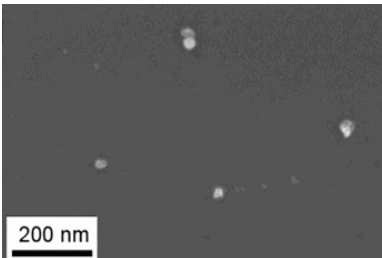
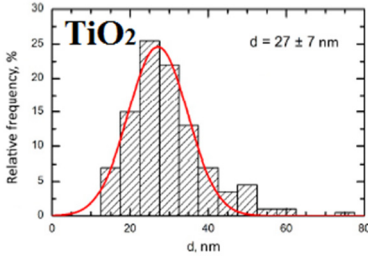
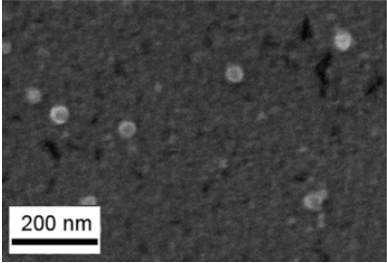
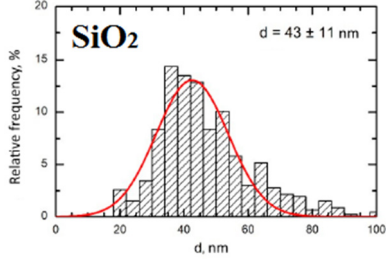
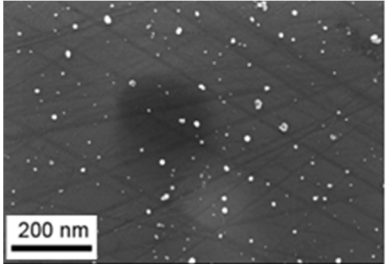
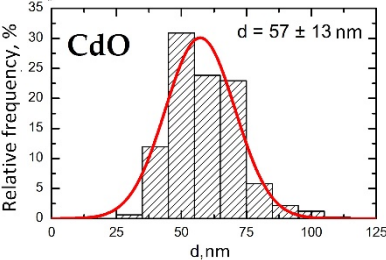
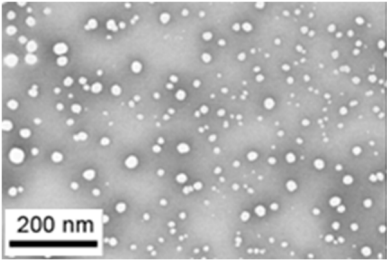
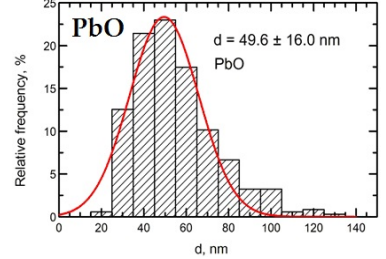
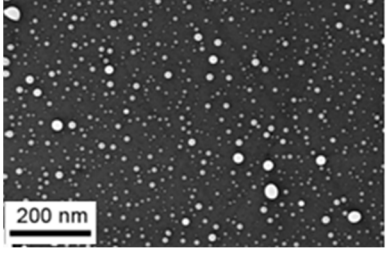
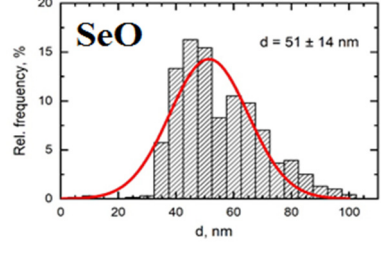
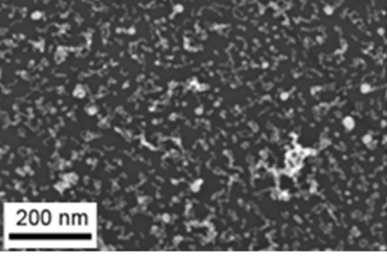
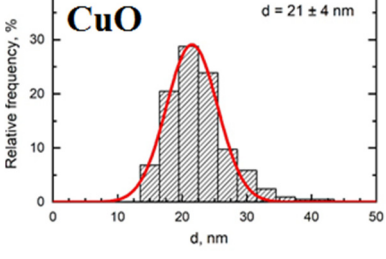
EO NPs, Size, nm	SEM Image of EO NPs in Suspension (x)	Particle Size Distribution Curve
Al_2O_3 21 ± 6		
TiO_2 27 ± 7		

Table 1. Cont.

EO NPs, Size, nm	SEM Image of EO NPs in Suspension (x)	Particle Size Distribution Curve
SiO ₂ 43 ± 11		
CdO 57 ± 13		
PbO 50 ± 16		
SeO 51 ± 14		
CuO 21 ± 4		

After exposure cessation, blood samples were taken by cervical dislocation during euthanasia and then tested for creatine kinase, uric acid, urea, and creatinine in blood serum, using Cobas Integra 400 plus automated analyzer (Roche Diagnostics GmbH, Germany) with appropriate test kits: CK Creatine Kinase COBAS INTEGRA/cobas c system, UA2 Uric Acid ver.2 COBAS INTEGRA/cobas c system, UREAL Urea BUN COBAS INTEGRA/cobas

c system, and CREJ2 Creatinine Jaffe Gen. 2 COBAS INTEGRA/cobas c system (Roche Diagnostics GmbH).

Table 2. Toxicity modeling in in vivo experiments.

AE	Group	Animals, <i>n</i>	Pre-Exposure Animal Body Weight, g	Injected Volume (mL), and Concentrations (mg/mL)	Total Dose of EO NPs Received	Local Ethics Committee Protocol No.
1	Control	12	292.27 ± 5.02	1 mL DIW	0 mg/kg	No. 62 of 1 February 2017
	Al ₂ O ₃	12	289.55 ± 7.93	0.25 mg/mL	18 mg/kg	
	TiO ₂	12	287.50 ± 7.40	0.5 mg/mL	36 mg/kg	
	SiO ₂	12	285.91 ± 9.17	0.5 mg/mL	36 mg/kg	
2	Control	12	217.50 ± 7.57	2 mL DIW	0 mg/kg	No. 2 of 1 February 2018
	CdO	12	217.50 ± 6.36	0.2 mL of 0.25 mg/mL NP suspension (per 200 g BW, i.e., 0.25 mg/kg BW of NPs) + 1.8 mL DIW	4.5 mg/kg	
	PbO	12	222.75 ± 6.38	1 mL of 0.5 mg/mL NP suspension (per 200 g BW, i.e., 2.5 mg/kg BW of NPs) + 1 mL DIW	45 mg/kg	
3	Control	12	239.17 ± 4.12	4 mL DIW	0 mg/kg	No. 2 of 20 April 2021
	SeO	12	225.91 ± 3.62	2 mL of 0.25 mg/mL NP suspension + 2 mL DIW	36 mg/kg	
	CuO	12	230.67 ± 2.91	2 mL of 0.25 mg/mL NP suspension + 2 mL DIW	36 mg/kg	

Abbreviations: AE, animal experiment; DIW, deionized water; BW, body weight; NP, nanoparticles.

The animals were dissected immediately after euthanasia, and their kidneys were visually examined and weighed. Imprint smears were made from fresh kidney sections and stained with Leishman for air-dried smears. The cellular composition and signs of cell damage were assessed using a Carl Zeiss Primo Star binocular microscope with a USCMOS video camera imaging system at 100× and 1000× magnification. During the microscopy, 300 cells from the imprint were counted.

Histological specimens were prepared by immersing kidneys in formalin and then cutting them into 2–3 mm thick slices treated with alcohols of increasing concentration and embedding in paraffin. Then, 3–4 µm sections were cut from the embedded blocks and stained with hematoxylin and eosin; in addition, the method of periodic acid–Schiff stain was also used. The study of histological preparations and their microphotography and morphometry were carried out using the Avtandilov ocular measuring grid and a computer software for pattern recognition, using an Olympus CX-41 microscope with an Olympus Soft Imaging Solution GMBH, Model LC20 camera, and LCmicro software. At least 30 measurements of each indicator were taken on preparations of four rodents from each exposure and the control groups.

Statistical analyses were performed using SPSS software (IBM Corp. Released 2021. IBM SPSS Statistics for Windows, Version 28.0. IBM Corp., Armonk, NY, USA). Groups were compared using one-way analysis of variance (ANOVA), followed by a normality check with the Shapiro–Wilk test. Post hoc comparisons were performed using the Bonferroni test. A *p*-value ≤ 0.05 was considered significant.

3. Results

In the absence of significant changes in the body weight (BW) of exposed animals compared to controls, the kidney weight showed a statistically significant decrease in those administered Al₂O₃ NPs (by 8% in proportion to BW); it showed an increase in those exposed to PbO NPs (by 9% of the absolute weight); and it remained unchanged following the exposure to SeO, CuO, TiO₂, SiO₂, and CdO NPs in the corresponding experiments.

The administration of SiO₂ and SeO NPs significantly reduced concentrations of urea and creatinine in blood serum, respectively (Table 3 and Appendix A Table A1).

No statistically significant changes were observed in the 24-h urine volumes and pH values (Table 1) in any group. However, we observed a statistically significant decrease in urinary total protein under the effect of CuO NPs and an increase in creatinine and urea concentrations after subchronic exposure to Al₂O₃ NPs (Table 3 and Appendix A Table A1). The comparative analysis of biochemical test results showed that Al₂O₃ NPs had the most pronounced nephrotoxic effect.

The morphological picture of kidneys in control animals from all experimental studies corresponded to the histological norm: the epithelium of convoluted tubules of the kidney had a clear periodic acid–Schiff (PAS) positive brush border on the apical side, homogenous cytoplasm, and optically clear nuclei (Figure 1). At the same time, we observed such dystrophic changes of various severity as dilated tubular lumens and deformed glomeruli in the exposed animals.

Table 3. Relative changes in blood serum and urine parameters in rats following the exposure to selected element oxide nanoparticles compared to controls of the corresponding animal experiment, %.

Parameter	Element Oxide Nanoparticles						
	Al ₂ O ₃	TiO ₂	SiO ₂	CdO	PbO	SeO	CuO
Serum Creatinine	↑0.6 (0.942)	↓11.59 (0.116)	↓7.00 (0.365)	↑6.60 (0.289)	↑6.79 (0.937)	↓15.44 * (0.017)	↓1.22 (0.774)
Serum Urea, mmol/L	↓16.89 (0.120)	↓12.39 (0.337)	↓25.9 * (0.044)	↑25.43 (0.283)	↑25.43 (0.504)	↓13.19 (0.566)	↓17.14 (0.399)
Urine Total Protein, mg/L	↑56.84 * (0.033)	↑13.72 (0.572)	↑33.71 (0.481)	↑10.69 (0.608)	↓12.58 (0.602)	↑62.54 (0.659)	↓29.76 * (0.009)
24 h Total Excretion of Protein, mg	↑11.68 (0.623)	↑6.93 (0.926)	↓1.82 (0.912)	↑14.29 (0.384)	↑18.59 (0.286)	↓43.85 * (0.017)	↓50.42 * (0.006)
Urine Creatinine, mmol/L	↑63.05 * (0.007)	↑36.94 (0.159)	↑59.24 (0.195)	↑12.43 (0.329)	↓1.69 (0.390)	↓16.46 (0.335)	↓20.73 (0.793)
Urine Protein Creatinine ratios, mg/μg	↓0.58 (0.988)	↓15.09 (0.358)	↓17.92 (0.332)	↑10.09 (0.534)	↑6.42 (0.609)	↓30.43 (0.098)	↓50.31 * (0.019)
Urine Urea, mmol/L	↑39.30 * (0.024)	↑21.26 (0.363)	↑37.23 (0.347)	↑11.70 (0.096)	↑12.10 (0.324)	↑29.35 (0.410)	↓67.89 (0.058)

Note: * Statistically different from the control groups (*p* in brackets, based on Student's *t*-test), ↓—decrease, ↑—increase.

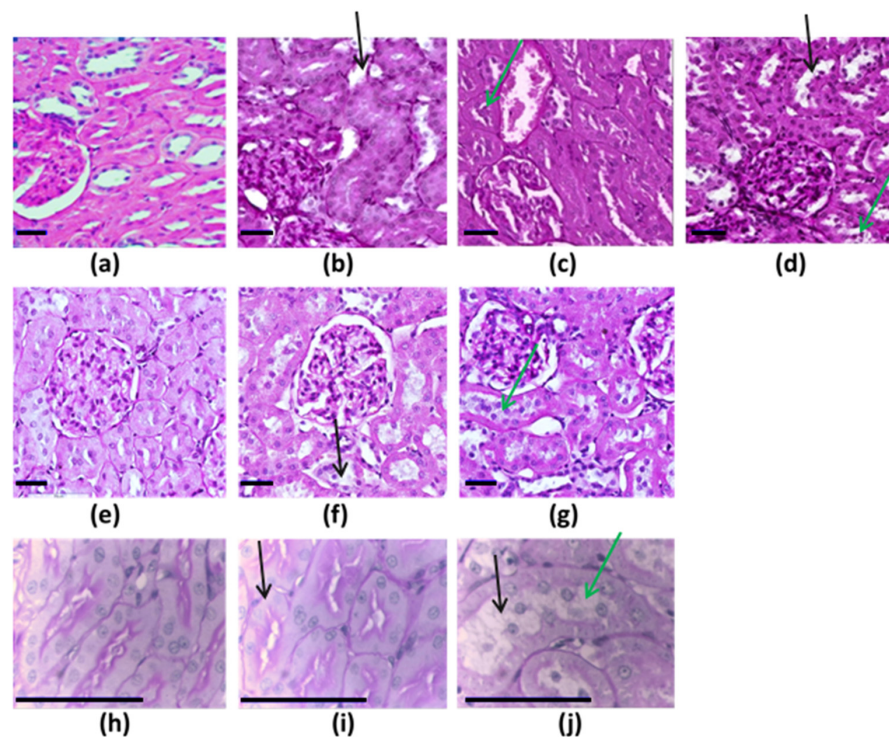


Figure 1. Histological picture of kidneys in control and EO-NP-exposed animals, periodic acid–Schiff staining, a 90× magnification for top and middle rows, and 400× magnification for bottom row. (a) Controls in the experiment with Al₂O₃, TiO₂ and SiO₂ NPs; animals exposed to (b) Al₂O₃ NPs, (c) TiO₂ NPs, and (d) SiO₂; (e) controls in the experiment with CdO and PbO NPs; animals exposed to (f) CdO NPs and (g) PbO NPs; (h) controls in the experiment with SeO and CuO NPs; and animals exposed to (i) SeO NPs and (j) CuO NPs. Black scale bars—35 μm. The black arrow points at dilated renal tubules, and the green arrow marks pronounced dystrophic and necrobiotic changes.

The histomorphological evaluation of the kidney tissues of animals exposed to EO NPs showed dystrophic changes of varying severity in the renal tubular epithelium: from the destruction of the brush border of epithelial cells to areas of necrobiosis/desquamation on the epithelium. Differences in morphometric parameters with the control animals were statistically significant in almost all groups (Figures 2 and 3). Cytological lesions were observed in all experimental groups following exposure to NPs (Table 4) and assessed in kidney imprint smears. A significantly larger proportion of lesions was found in proximal, rather than in distal, parts of the tubules.

Table 4. Proportion of cells of different types in rat kidney imprint smears following exposure to element oxide nanoparticles, % ($\bar{X} \pm$ s.e.).

Exposure Group	Renal Proximal Tubular Epithelial Cells	Degenerated Cells of Proximal Tubules	Renal Distal Tubular Epithelial Cells	Degenerated Cells of Distal Tubules	Neutrophils	Eosinophils
Animal Experiment with Al ₂ O ₃ , TiO ₂ , and SiO ₂ Nanoparticles						
Al ₂ O ₃ NPs	60.33 ± 2.82	13.00 ± 1.94	7.00 ± 1.47	8.33 ± 1.60	4.33 ± 1.18	2.33 ± 0.87
TiO ₂ NPs	56.00 ± 2.87 *	14.00 ± 2.00	7.67 ± 1.54	8.33 ± 1.60	5.00 ± 1.26	5.00 ± 1.26 *
SiO ₂ NPs	56.67 ± 2.86 *	14.67 ± 2.04	9.00 ± 1.65	6.00 ± 1.37	5.67 ± 1.33	2.00 ± 0.81
Deionized Water (Control)	67.67 ± 2.70	10.00 ± 1.73	7.67 ± 1.54	5.00 ± 1.26	5.00 ± 1.26	0.67 ± 0.47
Animal Experiment with PbO and CdO Nanoparticles						
PbO NPs	69.20 ± 1.66 *	9.80 ± 0.66 *	6.83 ± 0.48 *	5.00 ± 0.58	5.00 ± 0.73 *	3.33 ± 0.95
CdO NPs	69.17 ± 1.38 *	8.33 ± 1.33 *	9.20 ± 0.37	4.67 ± 0.42	2.50 ± 0.43	1.50 ± 0.22
Deionized Water (Control)	75.00 ± 1.38	4.20 ± 0.37	9.00 ± 0.71	4.20 ± 0.37	2.40 ± 0.40	1.80 ± 0.58
Animal Experiment with SeO and CuO Nanoparticles						
SeO NPs	51.50 ± 1.45 *	17.33 ± 0.99 *	8.17 ± 0.60 *	6.83 ± 0.48 *	6.83 ± 0.48	4.33 ± 0.49 *
CuO NPs	55.67 ± 0.84 *	14.67 ± 0.49 *	8.33 ± 0.56*	6.67 ± 0.33 *	5.50 ± 0.43	4.33 ± 0.42 *
Deionized Water (Control)	64.33 ± 1.26	6.33 ± 0.49	11.33 ± 0.88	5.00 ± 0.58	5.50 ± 0.56	2.67 ± 0.33

Note: * Statistically different from the control group ($p < 0.05$, based on Student's *t*-test).

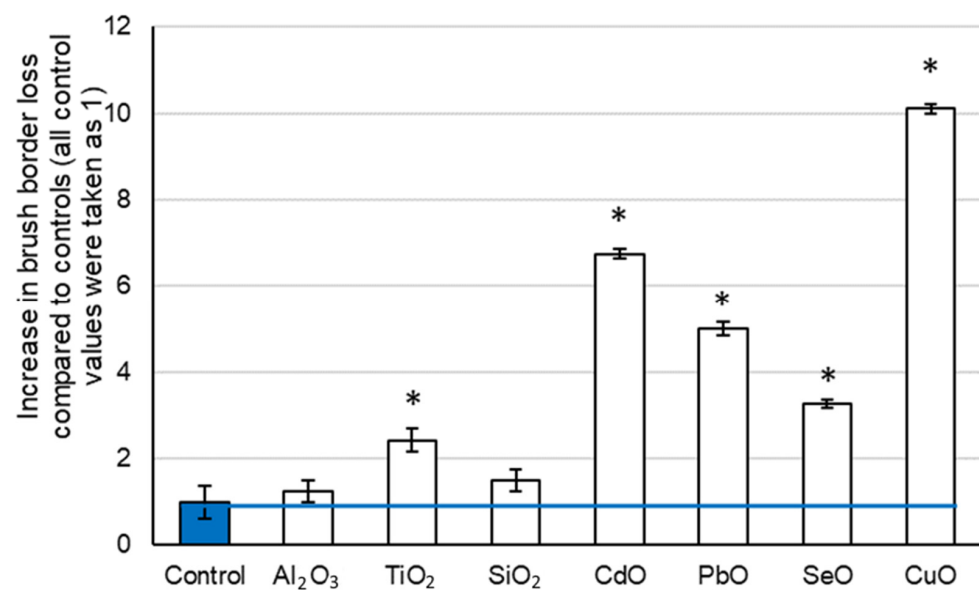


Figure 2. Loss of the brush border in rat kidney tissues following exposure to selected element oxide nanoparticles compared to the controls; the value of the indicator in each control group was taken as 1; values of the indicator in other groups were normalized to the control. Statistically significant difference from the corresponding values in *—control group ($p < 0.05$ via Student's *t*-test).

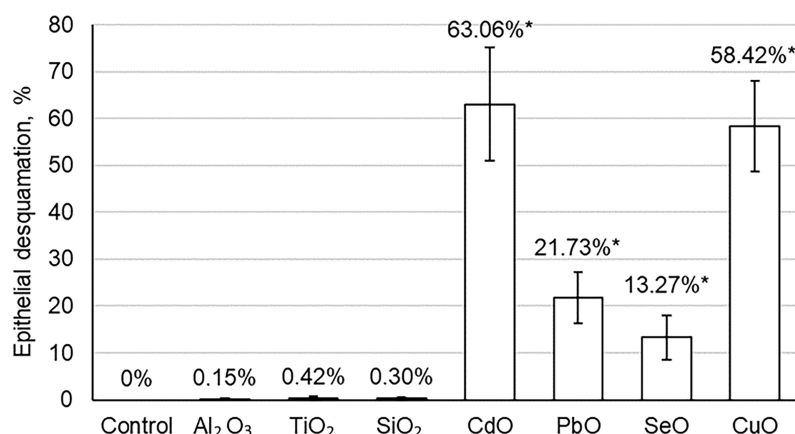


Figure 3. Percentage of desquamated epithelial cells in the kidneys of the rats exposed to selected element oxide nanoparticles compared to controls. Statistically significant difference from the corresponding values in *—control group ($p < 0.05$ via Student's *t*-test).

4. Discussion

The current scientific literature presents several experimental studies on the damaging effect of NPs on the structure and function of the testes and kidneys following exposure through different routes [20–30,34]. Male rodents' *in vitro* and *in vivo* reproductive toxicity caused by different types of inorganic NPs (AgNPs, AuNPs, IONPs, ZnONPs, TiO₂NPs and NiNPs) was recently evaluated in a systematic review of data published in the last twelve years. Structural and functional alterations were commonly observed in Sertoli, Leydig, germ, and sperm cells *in vitro* and *in vivo*. Oxidative stress, apoptosis, and/or necrosis were the most common findings after inorganic NP exposure. The toxicity of different NPs depends strongly on their physicochemical characteristics/intrinsic properties [34]. An oral route for 20 days of NPs of nano-silicon dioxide (nano-SiO₂) at a dose of 600 and 900 mg/kg/day was found to induce hyperemia in the kidney [21]. The study of a silver selenide nanocomposite at a dose of 500 µg/kg revealed swelling of renal convoluted tubules and, as a consequence, the compression of renal glomeruli and the proliferation of connective tissue in the interstitial space of renal tubules, a typical sign of kidney sclerosis [22]. Histological alterations in kidneys have been shown following a 28-day oral administration of iron oxide NPs. A higher concentration (1000 µg/kg) induced the dystrophy of convoluted tubules and a plethora of vessels of the renal cortex and glomeruli [23]. A morphological study of kidneys in rats orally exposed to Au NPs showed no significant differences between the animals administered NPs of different sizes: all of them developed dystrophy of renal tubular epithelium and focal cell necrosis. In addition, such changes in the lumen of convoluted tubules as a narrowing, stellate appearance and desquamated epithelium (in some fields of view) were observed, along with a moderate expansion of capillary loops of the glomeruli and plasma impregnation in small arterioles [24]. Other authors demonstrated the development of hyperemia of the renal tubules in Wistar rats after a 7-day oral administration of chromium oxide NPs at a dose of 500 µg/kg, as well as the cellularity of glomerular capillaries on day 14. The dose of 2000 µg/kg administered during the 7 days caused tubular hyperemia, as well as focal tubular atrophy and necrosis of the tubular epithelium. The histological picture observed following 14 days of a high-dose exposure was characterized by alterations in the kidney architecture, as evidenced by thickened capillary walls and the obliteration of the Bowman's capsule [25]. Inhalation exposure of mice to lead NPs at a concentration of 0.956×10^6 NPs/cm³, yielding a total dose of 1.684 µg/g body weight, over 11 weeks showed the highest accumulation of lead in the kidneys, while their histological examination revealed large lipid vacuoles in some blood vessels. The renal tubules that were closely adjacent to such vessels were compressed and showed damage to the epithelial membrane. Accumulations of lead NPs were found in the epithelial cells of proximal renal tubules [26].

The 7-day oral exposure to ultrafine lead oxide NPs at doses of 5 mg/kg and 10 mg/kg induced the loss of renal cell architecture and the narrowing of the inner diameter of both proximal and distal convoluted tubules [27].

Thus, in most studies, exposure to inorganic nanoparticles, regardless of the route of administration, led to structural and functional kidney disorders, among which oxidative stress, apoptosis and/or necrosis, hyperemia, and the destruction of the epithelium were most often described.

Kidneys are the main organ for the elimination of toxicants from the bloodstream [13]. NPs are known to increase oxidative stress by promoting the formation of reactive oxygen species [35]. Alterations in oxidative stress markers in the blood of animals (increased MDA and decreased catalase activity) were observed to a certain extent after exposure to all NPs examined [15,30–33]. Our studies aimed at showing the universal danger of NPs. Not all of the chemicals tested exert a toxic effect in their soluble form. Selenium, for instance, is an essential element in the physiological range of doses [33]. Titanium compounds have no adverse renal effects [36]. At the same time, inorganic compounds of aluminum [37], silicon [38], lead [39], cadmium [40,41], and copper [42] are nephrotoxic. However, they are all toxic in the form of NPs. In our research, all NPs were found to have a certain nephrotoxic effect. Biochemical, cytomorphological, and histological parameters did not always change in an interconnected manner, a fact that somewhat complicates the comparative assessment of the nephrotoxic effects of the nanosized particles under study.

According to the number of parameters of rats' urine and serum (urine pH shift to the acidic side and an increase in the content of protein, urea, uric acid, and creatinine in it at reduced mass coefficients of both kidneys), the Al₂O₃ NPs' effect was the most pronounced compared to that of other NPs administered, despite a relatively low dose of these NPs, which indirectly indicates their greater toxicity compared to TiO₂, SiO₂, CuO, and SeO NPs. Titanium dioxide NPs at doses of 300 mg/kg body weight (by gavage for 3 weeks) caused a 2- and 1.6-fold increase in concentrations of urea and serum creatinine, respectively [20]. We observed a similar, yet weaker, increase due to a significantly lower dose of NPs. We found a decrease in serum urea and creatinine after all NPs (excluding CdO and PbO NPs). It may indicate an increasing glomerular filtration rate. Previously, after exposure to SiO₂ NPs, hyperemia was shown [21]. It may be associated with an increased glomerular filtration rate and a decrease in serum urea and creatinine, which we observed in our study. A chronic increase in the glomerular filtration rate is a known cause of glomerulosclerosis and eventually leads to the loss of kidney function. However, the loss of kidney function has not taken place in our study.

It is worth noting that an even lower dose of CdO NPs, as well as the highest dose of PbO NPs, caused no significant changes in urine and serum parameters in rats compared to other NPs. PbO NPs increased both the absolute and relative weight of kidneys. We assume that NPs of the elements less demanded by the body have led to lesser changes in the urine and blood of rats due to the absence of natural mechanisms for the entry of nonessential metal ions into the cell. The size of nanoparticles is known to affect their toxicity, but an inverse monotonic relationship between them has not been shown by all nanoparticles. Even the finest nanoparticles (<10 nm) do not always demonstrate the highest toxicity. In the range from 10 to 100 nm, toxicity also often changes nonmonotonically [43,44]. Easy cellular uptake of NPs related to their size has been demonstrated [45]. It is believed that nanoparticles ≥ 50 nm are more easily recognized by defense systems of the body, which attenuates their toxic effect [43]. In our study, however, no such trend was observed, because rather large CdO and PbO NPs demonstrated more pronounced nephrotoxicity than smaller Al₂O₃ and TiO₂ NPs.

A statistically higher percentage of brush border loss in the rats exposed to TiO₂ NPs compared to the control animals, in contrast to those exposed to Al₂O₃ and SiO₂ NPs, was detected in the present study (Figure 2 and Appendix A Table A2). The same trend was noticeable in terms of epithelial desquamation (Figure 3 and Appendix A Table A2). If minimal changes in the histomorphometric parameters of the kidneys in rats exposed to

Al₂O₃ NPs can be partly explained by their lower dose, then in this trinity, TiO₂ NPs are the most nephrotoxic in terms of histomorphometric parameters.

Experimental animals exposed to PbO and CdO NPs demonstrated an even greater loss of the brush border. Cadmium and lead are known nephrotoxic poisons [40,41,46–48], and both of these metals are nonessential elements, so we expected to observe toxic damage to the kidneys after the cessation of exposure. The diameter of the renal glomeruli statistically decreased to the greatest extent (by 17.9%) in the rats exposed to PbO NPs ($32.90 \pm 1.01 \mu\text{m}$ against $40.08 \pm 1.09 \mu\text{m}$ in the controls, $p < 0.05$), but tubular epithelium was more damaged in those exposed to CdO NPs, as seen by the loss of the brush border and desquamation of the epithelium both on histological slides and cytological changes on smear preparations (Figures 2 and 3, Table 4, and Appendix A Table A2). The cell counts in imprint smears also indicated damage to the proximal rather than distal tubules.

In the experiment with SeO NPs and CuO NPs, a histological and cytomorphological assessment of their effects showed the greatest loss of the brush border induced by CuO NPs (Figure 2 and Appendix A Table A2). At the same time, the cytomorphological parameters showed a slightly greater deviation from the control values in the SeO NP exposure group (Table 4).

CuO NPs have a larger surface area and dissolve quickly, and dissolved copper easily changes its oxidation state [49]. All of these properties of CuO NPs lead to a sharp increase in oxidative stress in all organs of penetration, including the kidneys. NPs can be potentially excreted through kidneys, being transported outside the filtering glomerulus directly to the renal tubule [50,51].

Kidneys play an important role in selenium homeostasis [41,52]. Selenium is often used as a protector against nephrotoxic effects of chemicals (e.g., [53–57]). However, it has been shown that rising doses of Se NPs have an increasingly pronounced nephrotoxic effect and accumulate in renal tissues [58].

The results of cytology tests of kidney imprint smears (Table 4) were similar to those of the histological examination in terms of damages observed in all experimental groups (Figures 2 and 3 and Appendix A Table A2). Damage is seen in the cells of the proximal (rather than distal) convoluted tubules, but at the same time, toxic inflammation of this organ is again indicated mainly by the eosinophilic reaction in cytological imprint smears.

It is most likely that these metals exert a toxic effect on kidneys not so much in the form of persistent EO NPs, but rather in the form of ions released in the course of particle dissolution in biological fluids. Therefore, it can be assumed that the particular nephrotoxicity of TiO₂ NPs compared with Al₂O₃ and SiO₂ NPs is explained by its highest solubility, which was shown when fetal bovine serum was added in vitro to each nanosuspension [15]. After the partial dissolution of NPs, their toxic effects are attributed to the damaging effect of the remaining undissolved NPs, on the one hand, and that of the dissolved ions of chemical elements on the other. In fact, a nanoparticle is, on the one hand, a damaging agent itself and, on the other, a long-term source of ions of a chemical element that makes up its core. Regarding the element oxide NPs tested, it is worth noting the nephrotoxicity of soluble forms of aluminum, silicon, and copper described elsewhere [59–61]. At the same time, selenium in a narrow dose range was used to attenuate As- or Cd-mediated toxicity in kidneys [62]. Titanium derivatives showed no signs of nephrotoxicity [15], were widely studied [63–65], and are now used in anticancer therapy [66]. Undissolved NPs are transported in the bloodstream to organs and tissues, thus reaching the kidneys. The relocation of nanoparticles from lungs to kidneys and liver has been observed following inhalation exposure to lead oxide nanoparticles in mice [67].

On the whole, we evaluated 19 parameters of the excretory system following the exposure to Al₂O₃, TiO₂, SiO₂, PbO, CdO, CuO, and SeO NPs. Compared to the controls, we observed statistically significant alterations in 42.1% (8 of 19) of parameters following the exposure to PbO, CuO, and SeO NPs, in 21.1% (4 of 19)—following that to CdO and Al₂O₃ NPs—and in 15.8% (3 of 19) and 10.5% (2 of 19) of indicators following the exposures to TiO₂ and SiO₂ NPs, respectively.

Although a direct comparison of nanoparticle nephrotoxicity in our study is impractical due to different doses under study, it is worth mentioning that PbO, CuO, and SeO NPs were found to have the most pronounced nephrotoxic effect, as judged by the alterations induced. It is of particular interest that the dose of CuO or SeO NPs was lower than that of PbO NPs, but their toxic effects were comparable.

Summarizing our findings, it is worth noting that, regardless of the chemical nature, element oxide NPs have a nephrotoxic effect and cause more damage to proximal (rather than distal) parts of renal tubules.

The common mechanisms of renal damage following the exposure of NPs of any chemical nature include an increase in oxidative stress, accumulations and penetrations of NPs into cells and damage to the intracellular structures, and toxic effects of chemical elements composing NPs after dissolution in biological fluids. Understanding the mechanisms of the renal toxicity of NPs can facilitate early diagnosis of occupational nephropathies, thus enabling timely treatment, slowing down the disease progression, and prolonging the human work capacity.

5. Conclusions

NPs generated as by-products in many industrial processes seem to be particularly dangerous to organs such as the testes and the kidneys. All element oxide NPs under investigation that were instilled intraperitoneally demonstrated a nephrotoxic effect, following subchronic exposure, in the present study. Unambiguous ranking of the NPs examined by the degree of their nephrotoxicity is difficult. The severity of cyto- and histological structural changes in kidneys depends on the chemical nature of NPs. These alterations are not always consistent with biochemical ones, thus impeding early clinical diagnosis of renal changes.

Additional profound research is necessary to establish molecular genetic aspects of exposure to nanoparticles of a different chemical nature, with a different accumulation and dissolution of nanoparticles in kidneys and other organs and different mechanisms of the cellular uptake of nanoparticles and their dissolved ions. It can also facilitate the identification of key indicators of nephrotoxic effects contributing to the early diagnosis of NP-induced occupational and nonoccupational nephropathies.

Author Contributions: Conceptualization, I.A.M., M.P.S. and B.A.K.; investigation, S.V.K. (Svetlana V. Klinova), Y.V.R., I.E.V., E.M.P. and A.K.T.; writing—original draft preparation, S.V.K. (Svetlana V. Klinova), Y.V.R. and A.K.T.; writing—review and editing, I.A.M., M.P.S., L.I.P., A.M.T., C.M., K.S. and S.V.K. (Svetlana V. Klinova); visualization, S.V.K. (Sergey V. Kuzmin), A.K.T. and I.E.V.; supervision, M.P.S., L.I.P. and A.M.T.; project administration, I.A.M. All authors have read and agreed to the published version of the manuscript.

Funding: This research received no external funding.

Institutional Review Board Statement: The animal study protocols were approved by the Institutional Ethics Committee of the Yekaterinburg Medical Research Center for Prophylaxis and Health Protection in Industrial Workers (Protocol No. 62 of 20 January 2017, Protocol No. 2 of 1 February 2018, and Protocol No. 2 of 20 April 20).

Informed Consent Statement: Not applicable.

Data Availability Statement: The data presented in this study are available on request from the corresponding author.

Acknowledgments: The authors would like to express their sincere gratitude to the personnel of the Ural Center for Collective Use “Modern Nanotechnologies” of the Ural Federal University named after the First President of Russia, B.N. Yeltsin, and personally to its director, Vladimir Ya. Shur, for the synthesis of specific suspensions of nanoparticles.

Conflicts of Interest: The authors declare no conflict of interest.

Appendix A

Table A1. Some functional parameters of the excretory system of rats following 18 repeated intraperitoneal injections of suspensions of Al₂O₃, TiO, SiO, PbO, CdO, SeO, and CuO nanoparticles for six weeks ($\bar{X} \pm S.e.$).

Index	Exposure Group									
	Deionized Water (Control)	Al ₂ O ₃ NPs	TiO ₂ NPs	SiO ₂ NPs	Deionized Water (Control)	PbO NPs	CdO NPs	Deionized Water (Control)	SeO NPs	CuO NPs
Kidney Weight, g	1.99 ± 0.04	1.89 ± 0.04	2.01 ± 0.04	1.97 ± 0.02	1.85 ± 0.05	2.02 ± 0.06 *	1.88 ± 0.08	1.73 ± 0.04	1.85 ± 0.09	1.68 ± 0.06
Kidney Weight, g/100 g Body Weight	0.61 ± 0.01	0.56 ± 0.01 *	0.60 ± 0.01	0.60 ± 0.01	0.60 ± 0.01	0.66 ± 0.01 *	0.61 ± 0.02	0.44 ± 0.08	0.47 ± 0.08	0.43 ± 0.08
Uric Acid in Blood Serum, μmol/L	120.50 ± 10.86	154.88 ± 13.53	135.50 ± 15.29	128.25 ± 17.67	86.53 ± 6.91	87.43 ± 4.60	92.93 ± 8.08	132.50 ± 12.37	106.00 ± 13.42	153.43 ± 29.47
Serum Urea, mmol/L	4.44 ± 0.34	3.69 ± 0.28	3.89 ± 0.45	3.29 ± 0.40 *	4.64 ± 0.59	5.82 ± 0.68	5.82 ± 0.77	4.55 ± 0.75	3.95 ± 0.68	3.77 ± 0.52
Serum Creatinine, μmol/L	34.84 ± 2.09	35.05 ± 1.78	30.80 ± 0.71	32.40 ± 1.29	37.84 ± 2.35	40.34 ± 3.46	40.41 ± 2.52	39.18 ± 1.63	33.13 ± 1.35*	38.70 ± 0.63
Clearance of Endogenous Creatinine, mL/min	1.40 ± 0.15	1.58 ± 0.18	1.90 ± 0.24	1.74 ± 0.19	1.16 ± 0.08	1.12 ± 0.08	1.14 ± 0.11	1.32 ± 0.09	1.40 ± 0.12	1.53 ± 0.08
24 h Urine Volume, mL	29.67 ± 4.36	18.14 ± 3.63	26.43 ± 3.88	28.43 ± 5.73	26.47 ± 2.75	20.30 ± 3.02	25.50 ± 2.09	25.50 ± 4.63	14.29 ± 4.94	24.38 ± 4.99
Urine Protein, mg/L	190.43 ± 29.63	298.45 ± 32.35 *	216.55 ± 33.41	254.63 ± 76.97	222.41 ± 26.87	246.19 ± 31.59	194.43 ± 17.90	232.16 ± 16.08	377.35 ± 147.54	163.05 ± 12.33 *
24 h Total Excretion of Protein, mg	5.48 ± 1.14	6.12 ± 0.67	5.86 ± 0.66	5.38 ± 0.71	5.11 ± 0.65	5.84 ± 0.64	6.06 ± 0.64	7.16 ± 0.62	4.02 ± 1.03 *	3.55 ± 0.72 *
Urine Creatinine, μmol/L	1.57 ± 0.11	2.56 ± 0.27 *	2.15 ± 0.35	2.50 ± 0.61	1.77 ± 0.17	1.99 ± 0.19	1.74 ± 0.12	1.64 ± 0.15	1.37 ± 0.07	1.30 ± 0.06
Urine Protein Creatinine ratios, mg/μg	1.06 ± 0.14	1.06 ± 0.11	0.90 ± 0.04	0.87 ± 0.07	1.09 ± 0.07	1.20 ± 0.09	1.16 ± 0.11	1.61 ± 0.27	1.12 ± 0.18	0.80 ± 0.13 *
Urine Urea, mmol/L	229.30 ± 16.00	319.41 ± 29.85 *	278.06 ± 46.97	314.67 ± 78.85	227.37 ± 18.53	253.98 ± 18.82	254.89 ± 21.77	209.06 ± 25.24	270.41 ± 61.87	141.94 ± 14.81
Uric Acid in Urine, μmol/L	234.00 ± 38.97	319.50 ± 45.51	292.50 ± 105.70	304.71 ± 93.85	205.86 ± 21.46	208.58 ± 13.10	226.15 ± 17.06	173.20 ± 9.36	173.33 ± 44.33	160.33 ± 6.17

Note: * Statistically different from the control group ($p < 0.05$, based on Student's t -test).

Table A2. Morphometric indices of damage to the epithelium of proximal convoluted tubules in rats following subchronic exposure to element oxide nanoparticles ($\bar{X} \pm S.e.$).

Index	Exposure Group									
	Deionized Water (Control)	Al ₂ O ₃ NPs	TiO ₂ NPs	SiO ₂ NPs	Deionized Water (Control)	PbO NPs	CdO NPs	Deionized Water (Control)	SeO NPs	CuO NPs
Brush Border Loss, %	1.49 ± 0.56	1.85 ± 0.47	3.61 ± 0.99 *	2.24 ± 0.58	6.70 ± 1.90	33.54 ± 5.44 *	45.18 ± 5.03 *	5.34 ± 0.65	17.39 ± 1.64 *	53.92 ± 5.41 *
Epithelial Desquamation, %	0.00 ± 0.00	0.15 ± 0.15	0.42 ± 0.36	0.30 ± 0.25	0.00 ± 0.00	21.73 ± 5.51 *	63.06 ± 12.09 *	0.00 ± 0.00	13.27 ± 4.75 *	58.42 ± 9.68 *

Note: * Statistically different from the control group ($p < 0.05$, based on Student's t -test).

References

1. Hill, N.R.; Fatoba, S.T.; Oke, J.L.; Hirst, J.A.; O'Callaghan, C.A.; Lasserson, D.S.; Hobbs, F.D.R. Global Prevalence of Chronic Kidney Disease—A Systematic Review and Meta-Analysis. *PLoS ONE* **2016**, *11*, e0158765. [CrossRef]
2. GBD Chronic Kidney Disease Collaboration. Global, regional, and national burden of chronic kidney disease, 1990–2017: A systematic analysis for the Global Burden of Disease Study. *Lancet* **2017**, *395*, 709–733.
3. Liyanage, T.; Toyama, T.; Hockham, C.; Ninomiya, T.; Perkovic, V.; Woodward, M.; Fukagawa, M.; Matsushita, K.; Praditpornsilpa, K.; Hooi, L.S.; et al. Prevalence of chronic kidney disease in Asia: A systematic review and analysis. *BMJ Glob. Health* **2022**, *7*, e007525. [CrossRef]
4. Jubber, I.; Ong, S.; Bukavina, L.; Black, P.C.; Comp erat, E.; Kamat, A.M.; Kiemeny, L.; Lawrentschuk, N.; Lerner, S.P.; Meeks, J.J.; et al. Epidemiology of Bladder Cancer in 2023: A Systematic Review of Risk Factors. *Eur. Urol.* **2023**, *84*, 176–190. [CrossRef]
5. Knapke, E.T.; Magalhaes, D.P.; Dalvie, M.A.; Mandrioli, D.; Perry, M.J. Environmental and occupational pesticide exposure and human sperm parameters: A Navigation Guide review. *Toxicology* **2022**, *465*, 153017. [CrossRef]
6. Amir, S.; Tzatzarakis, M.; Mamoulakis, C.; Bello, J.H.; Eqani, S.A.M.A.S.; Vakonaki, E.; Karavitakis, M.; Sultan, S.; Tahir, F.; Shah, S.T.A.; et al. Impact of organochlorine pollutants on semen parameters of infertile men in Pakistan. *Environ. Res.* **2021**, *195*, 110832. [CrossRef]
7. Amir, S.; Shah, S.T.A.; Mamoulakis, C.; Docea, A.O.; Kalantzi, O.I.; Zachariou, A.; Calina, D.; Carvalho, F.; Sofikitis, N.; Makrigiannakis, A.; et al. Endocrine Disruptors Acting on Estrogen and Androgen Pathways Cause Reproductive Disorders through Multiple Mechanisms: A Review. *Int. J. Environ. Res. Public Health* **2021**, *18*, 1464. [CrossRef]
8. Krstev, S.; Knutsson, A. Occupational Risk Factors for Prostate Cancer: A Meta-analysis. *J. Cancer Prev.* **2019**, *24*, 91–111. [CrossRef]
9. Georgiadis, G.; Mavridis, C.; Belantis, C.; Zisis, I.E.; Skamagkas, I.; Fragkiadoulaki, I.; Heretis, I.; Tzortzis, V.; Psathakis, K.; Tsatsakis, A.; et al. Nephrotoxicity issues of organophosphates. *Toxicology* **2018**, *406–407*, 129–136. [CrossRef]
10. Kalliora, C.; Mamoulakis, C.; Vasilopoulos, E.; Stamatiades, G.A.; Kalafati, L.; Barouni, R.; Karakousi, T.; Abdollahi, M.; Tsatsakis, A. Association of pesticide exposure with human congenital abnormalities. *Toxicol. Appl. Pharmacol.* **2018**, *346*, 58–75. [CrossRef]
11. Petrakis, D.; Vassilopoulou, L.; Mamoulakis, C.; Psycharakis, C.; Anifantaki, A.; Sifakis, S.; Docea, A.O.; Tsiaoussis, J.; Makrigiannakis, A.; Tsatsakis, A.M. Endocrine Disruptors Leading to Obesity and Related Diseases. *Int. J. Environ. Res. Public Health* **2017**, *14*, 1282. [CrossRef] [PubMed]
12. Dinca, V.; Docea, A.O.; Drocas, A.I.; Nikolouzakis, T.K.; Stivaktakis, P.D.; Nikitovic, D.; Golokhvast, K.S.; Hernandez, A.F.; Calina, D.; Tsatsakis, A. A mixture of 13 pesticides, contaminants, and food additives below individual NOAELs produces histopathological and organ weight changes in rats. *Arch. Toxicol.* **2023**, *97*, 1285–1298. [CrossRef] [PubMed]
13. P ocsi, I.; Dockrell, M.E.; Price, R.G. Nephrotoxic biomarkers with specific indications for metallic pollutants: Implications for environmental health. *Biomark. Insights* **2022**, *17*, 11772719221111882. [CrossRef]
14. Lentini, P.; Zanolli, L.; Granata, A.; Signorelli, S.S.; Castellino, P.; Dell'Aquila, R. Kidney and heavy metals—The role of environmental exposure (Review). *Mol. Med. Rep.* **2017**, *15*, 3413–3419. [CrossRef] [PubMed]
15. Minigalieva, I.A.; Katsnelson, B.A.; Privalova, L.I.; Sutunkova, M.P.; Gurvich, V.B.; Shur, V.Y.; Shishkina, E.V.; Valamina, I.E.; Makeyev, O.H.; Panov, V.G.; et al. Combined subchronic toxicity of aluminum (III), titanium (IV) and silicon (IV) oxide nanoparticles and its alleviation with a complex of bioprotectors. *Int. J. Mol. Sci.* **2018**, *19*, 837. [CrossRef]
16. Ahmad, T.; Ahmad, K.; Khan, Z.I.; Munir, Z.; Khalofah, A.; Al-Qthanin, R.N.; Alsubeie, M.S.; Alamri, S.; Hashem, M.; Farooq, S.; et al. Chromium accumulation in soil, water and forage samples in automobile emission area. *Saudi J. Biol. Sci.* **2021**, *28*, 3517–3522. [CrossRef]
17. Tumane, R.G.; Nath, N.; Khan, A. Risk Assessment in Mining-Based Industrial Workers by Immunological Parameters as Copper Toxicity Markers. *Indian J. Occup. Environ. Med.* **2019**, *23*, 21–27.
18. WHO: Lead Poisoning. Available online: <https://www.who.int/news-room/fact-sheets/detail/lead-poisoning-and-health> (accessed on 3 June 2023).
19. Mirkov, I.; Popov Aleksandrov, A.; Ninkov, M.; Tucovic, D.; Kulas, J.; Zeljkovic, M.; Popovic, D.; Kataranovski, M. Immunotoxicology of cadmium: Cells of the immune system as targets and effectors of cadmium toxicity. *Food Chem. Toxicol.* **2021**, *149*, 112026. [CrossRef]
20. Shirdare, M.; Jabbari, F.; Salehzadeh, M.; Ziamajidi, N.; Nourian, A.; Heidarisan, S.; Ghavimishamekh, A.; Taheri Azandariani, M.; Abbasalipourkabir, R. Curcuma reduces kidney and liver damage induced by titanium dioxide nanoparticles in male Wistar rats. *Avicenna J. Phytomedicine* **2022**, *12*, 537–547.
21. Firouzmandi, M.; Hejazy, M.; Mohammadi, A.; Shahbazfar, A.A.; Norouzi, R. In Vivo Toxicity of Oral Administrated Nano-SiO₂: Can Food Additives Increase Apoptosis? *Biol. Trace Elem. Res.* **2023**, *201*, 4769–4778. [CrossRef]
22. Titov, E.A.; Sosedova, L.M.; Novikov, M.A.; Zvereva, M.V.; Rukavishnikov, V.S.; Lakhman, O.L. The Analysis of Acute and Subacute Toxicity of Silver Selenide Nanoparticles Encapsulated in Arabinogalactan Polymer Matrix. *Polymers* **2022**, *14*, 3200. [CrossRef] [PubMed]
23. Kumari, M.; Rajak, S.; Singh, S.P.; Kumari, S.I.; Kumar, P.U.; Murty, U.S.; Mahboob, M.; Grover, P.; Rahman, M.F. Repeated oral dose toxicity of iron oxide nanoparticles: Biochemical and histopathological alterations in different tissues of rats. *J. Nanosci. Nanotechnol.* **2012**, *12*, 2149–2159. [CrossRef] [PubMed]
24. Sani, A.; Cao, C.; Cui, D. Toxicity of gold nanoparticles (AuNPs): A review. *Biochem. Biophys. Rep.* **2021**, *26*, 100991.

25. Fatima, R.; Akhtar, K.; Hossain, M.M.; Ahmad, R. Chromium oxide nanoparticle-induced biochemical and histopathological alterations in the kidneys and brain of Wistar rats. *Toxicol. Ind. Health* **2017**, *33*, 911–921. [[CrossRef](#)] [[PubMed](#)]
26. Smutná, T.; Dumková, J.; Kristeková, D.; Laštovičková, M.; Jedličková, A.; Vrlíková, L.; Dočekal, B.; Alexa, L.; Kotasová, H.; Pelková, V.; et al. Macrophage-mediated tissue response evoked by subchronic inhalation of lead oxide nanoparticles is associated with the alteration of phospholipases C and cholesterol transporters. *Part. Fibre Toxicol.* **2022**, *19*, 52. [[CrossRef](#)]
27. Kadammattil, A.V.; Sajankila, S.P.; Prabhu, S.; Rao, B.N.; Rao, B.S.S. Systemic toxicity and teratogenicity of copper oxide nanoparticles and copper sulfate. *J. Nanosci. Nanotechnol.* **2018**, *18*, 2394–2404. [[CrossRef](#)]
28. Piperigkou, Z.; Karamanou, K.; Engin, A.B.; Gialeli, C.; Docea, A.O.; Vynios, D.H.; Pavão, M.S.; Golokhvast, K.S.; Shtilman, M.I.; Argiris, A.; et al. Emerging aspects of nanotoxicology in health and disease: From agriculture and food sector to cancer therapeutics. *Food Chem. Toxicol. Int. J. Publ. Br. Ind. Biol. Res. Assoc.* **2016**, *91*, 42–57. [[CrossRef](#)]
29. Coricovac, D.E.; Moacă, E.A.; Pinzaru, I.; Cîtu, C.; Soica, C.; Mihali, C.V.; Păcurariu, C.; Tutelyan, V.A.; Tsatsakis, A.; Dehelean, C.A. Biocompatible Colloidal Suspensions Based on Magnetic Iron Oxide Nanoparticles: Synthesis, Characterization and Toxicological Profile. *Front. Pharmacol.* **2017**, *8*, 154. [[CrossRef](#)]
30. Minigalieva, I.A.; Katsnelson, B.A.; Panov, V.G.; Privalova, L.I.; Varaksin, A.N.; Gurchich, V.B.; Sutunkova, M.P.; Shur, V.Y.; Shishkina, E.V.; Valamina, I.E.; et al. In vivo toxicity of copper oxide, lead oxide and zinc oxide nanoparticles acting in different combinations and its attenuation with a complex of innocuous bio-protectors. *Toxicology* **2017**, *380*, 72–93. [[CrossRef](#)]
31. Sutunkova, M.P.; Minigalieva, I.A.; Klinova, S.V.; Panov, V.G.; Gurchich, V.B.; Privalova, L.I.; Sakhautdinova, R.R.; Shur, V.Y.; Shishkina, E.V.; Shtin, T.N.; et al. Some data on the comparative and combined toxic activity of nanoparticles containing lead and cadmium with special attention to their vasotoxicity. *Nanotoxicology* **2020**, *15*, 205–222. [[CrossRef](#)]
32. Klinova, S.V.; Katsnelson, B.A.; Minigalieva, I.A.; Gerzen, O.P.; Balakin, A.A.; Lisin, R.V.; Butova, K.A.; Nabiev, S.R.; Lookin, O.N.; Katsnelson, L.B.; et al. Cardioinotropic effects in subchronic intoxication of rats with lead and/or cadmium oxide nanoparticles. *Int. J. Mol. Sci.* **2021**, *22*, 3466. [[CrossRef](#)]
33. Bushueva, T.V.; Panov, V.G.; Minigalieva, I.A.; Privalova, L.I.; Vedernikova, M.S.; Gurchich, V.B.; Sutunkova, M.P.; Katsnelson, B.A. Dose dependence of the separate and combined impact of copper-oxide and selenium-oxide nanoparticles on oxygen consumption by cells in vitro with or without the background action of some modulators of the mitochondrial respiratory function. *Dose Response* **2023**, *21*, 15593258221106612. [[CrossRef](#)]
34. Dantas, G.P.F.; Ferraz, F.S.; Andrade, L.M.; Costa, G.M.J. Male reproductive toxicity of inorganic nanoparticles in rodent models: A systematic review. *Chem. Biol. Interact.* **2022**, *363*, 110023. [[CrossRef](#)] [[PubMed](#)]
35. Fu, P.P.; Xia, Q.; Hwang, H.M.; Ray, P.C.; Yu, H. Mechanisms of nanotoxicity: Generation of reactive oxygen species. *J. Food Drug Anal.* **2014**, *22*, 64–75. [[CrossRef](#)] [[PubMed](#)]
36. Burk, R.F.; Hill, K.E. Regulation of Selenium Metabolism and Transport. *Annu. Rev. Nutr.* **2015**, *35*, 109–134. [[CrossRef](#)]
37. Wei, H.; Li, D.; Luo, Y.; Wang, Y.; Lin, E.; Wei, X. Aluminum exposure induces nephrotoxicity via fibrosis and apoptosis through the TGF- β 1/Smads pathway in vivo and in vitro. *Ecotoxicol. Environ. Saf.* **2023**, *249*, 114422. [[CrossRef](#)] [[PubMed](#)]
38. Ghahramani, N. Silica nephropathy. *Int. J. Occup. Environ. Med.* **2010**, *1*, 108–115. [[PubMed](#)]
39. Kahalerras, L.; Otmami, I.; Abdennour, C. The Allium triquetrum L. leaves mitigated hepatotoxicity and nephrotoxicity induced by lead acetate in Wistar rats. *Biol. Trace Elem. Res.* **2022**, *200*, 4733–4743. [[CrossRef](#)]
40. Satarug, S.; Gobe, G.C.; Vesey, D.A.; Phelps, K.R. Cadmium and lead exposure, nephrotoxicity, and mortality. *Toxics* **2020**, *8*, 86. [[CrossRef](#)]
41. Desoize, B. Metals and metal compounds in cancer treatment. *Anticancer. Res.* **2004**, *24*, 1529–1544.
42. Peng, X.; Dai, C.; Zhang, M.; Das Gupta, S. Molecular mechanisms underlying protective role of quercetin on copper sulfate-induced nephrotoxicity in mice. *Front. Vet. Sci.* **2021**, *7*, 586033. [[CrossRef](#)] [[PubMed](#)]
43. Sukhanova, A.; Bozrova, S.; Sokolov, P.; Berestovoy, M.; Karaulov, A.; Nabiev, I. Dependence of nanoparticle toxicity on their physical and chemical properties. *Nanoscale Res. Lett.* **2018**, *13*, 44. [[CrossRef](#)] [[PubMed](#)]
44. Ali, M. What function of nanoparticles is the primary factor for their hypertoxicity? *Adv. Colloid Interface Sci.* **2023**, *314*, 102881. [[CrossRef](#)]
45. Matczuk, M.; Ruzik, L.; Aleksenko, S.S.; Keppler, B.K.; Jarosz, M.; Timerbaev, A.R. Analytical methodology for studying cellular uptake, processing and localization of gold nanoparticles. *Anal. Chim. Acta* **2019**, *1052*, 1–9. [[CrossRef](#)] [[PubMed](#)]
46. Cirovic, A.; Denic, A.; Clarke, B.L.; Vassallo, R.; Cirovic, A.; Landry, G.M. A hypoxia-driven occurrence of chronic kidney disease and osteoporosis in COPD individuals: New insights into environmental cadmium exposure. *Toxicology* **2022**, *482*, 153355. [[CrossRef](#)] [[PubMed](#)]
47. Dong, W.; Zhang, K.; Gong, Z.; Luo, T.; Li, J.; Wang, X.; Zou, H.; Song, R.; Zhu, J.; Ma, Y.; et al. N-acetylcysteine delayed cadmium-induced chronic kidney injury by activating the sirtuin 1–P53 signaling pathway. *Chem. Biol. Interact.* **2023**, *369*, 110299. [[CrossRef](#)] [[PubMed](#)]
48. Balmuri, S.R.; Selvaraj, U.; Kumar, V.V.; Anthony, S.P.; Tsatsakis, A.M.; Golokhvast, K.S.; Raman, T. Effect of surfactant in mitigating cadmium oxide nanoparticle toxicity: Implications for mitigating cadmium toxicity in environment. *Environ. Res.* **2017**, *152*, 141–149. [[CrossRef](#)] [[PubMed](#)]
49. Chaudhary, R.G.; Bhusari, G.S.; Tiple, A.D.; Rai, A.R.; Somkuvar, S.R.; Potbhare, A.K.; Lambat, T.L.; Ingle, P.P.; Abdala, A.A. Metal/metal oxide nanoparticles: Toxicity, applications, and future prospects. *Curr. Pharm. Des.* **2019**, *25*, 4013–4029. [[CrossRef](#)] [[PubMed](#)]

50. Naumenko, V.; Nikitin, A.; Kapitanova, K.; Melnikov, P.; Vodopyanov, S.; Garanina, A.; Valikhov, M.; Ilyasov, A.; Vishnevskiy, D.; Markov, A.; et al. Intravital microscopy reveals a novel mechanism of nanoparticles excretion in kidney. *J. Control Release* **2019**, *307*, 368–378. [[CrossRef](#)]
51. Tsatsakis, A.M. *Toxicological Risk Assessment and Multi-System Health Impacts from Exposure*; Tsatsakis, A.M., Ed.; Academic Press: Cambridge, MA, USA, 2021; p. 687.
52. Dworkin, B.; Weseley, S.; Rosenthal, W.S.; Schwartz, E.M.; Weiss, L. Diminished blood selenium levels in renal failure patients on dialysis: Correlations with nutritional status. *Am. J. Med. Sci.* **1987**, *293*, 6–12. [[CrossRef](#)]
53. Ryabova, Y.V.; Sutunkova, M.P.; Minigalieva, I.A.; Shabardina, L.V.; Filippini, T.; Tsatsakis, A. Toxicological effects of selenium nanoparticles in laboratory animals: A review. *J. Appl. Toxicol. JAT* **2023**. [[CrossRef](#)] [[PubMed](#)]
54. Zhang, X.; Wang, Q.; Zhang, J.; Song, M.; Shao, B.; Han, Y.; Yang, X.; Li, Y. The protective effect of selenium on T-2-induced nephrotoxicity is related to the inhibition of ROS-mediated apoptosis in mice kidney. *Biol. Trace Elem. Res.* **2022**, *200*, 206–216. [[CrossRef](#)] [[PubMed](#)]
55. Najmaddin, S.A.; Amin, Z.A. Adiantum capillus attained selenium nanoparticles (SeNPs) ameliorate resistive effects in rat model of gentamicin nephrotoxicity via regulation of Interlukin-1 β , tumor necrosis factor- α and engagement of Vimentin and Bcl-2 proteins. *Saudi J. Biol. Sci.* **2023**, *30*, 103550. [[CrossRef](#)] [[PubMed](#)]
56. Han, Q.; Wang, A.; Fu, Q.; Zhou, S.; Bao, J.; Xing, H. Protective role of selenium on ammonia-mediated nephrotoxicity via PI3K/AKT/mTOR pathway: Crosstalk between autophagy and cytokine release. *Ecotoxicol. Environ. Saf.* **2022**, *242*, 113918. [[CrossRef](#)] [[PubMed](#)]
57. Chen, H.; Zhang, Y.; Qi, X.; Shi, X.; Huang, X.; Xu, S.W. Selenium deficiency aggravates bisphenol A-induced autophagy in chicken kidney through regulation of nitric oxide and adenosine monophosphate activated protein kinase/mammalian target of rapamycin signaling pathway. *Environ. Toxicol.* **2022**, *37*, 2503–2514. [[CrossRef](#)]
58. Nagy, G.; Benko, I.; Kiraly, G.; Voros, O.; Tanczos, B.; Sztrik, A.; Takács, T.; Pócsi, I.; Prokisch, J.; Banfalvi, G. Cellular and nephrotoxicity of selenium species. *J. Trace Elem. Med. Biol.* **2015**, *30*, 160–170. [[CrossRef](#)]
59. Kaya, S.; Yalçın, T.; Boydak, M.; Dönmez, H.H. Protective effect of n-acetylcysteine against aluminum-induced kidney tissue damage in rats. *Biol. Trace Elem. Res.* **2023**, *201*, 1806–1815. [[CrossRef](#)]
60. Mourad, B.H.; Ashour, Y.A. Demonstration of subclinical early nephrotoxicity induced by occupational exposure to silica among workers in pottery industry. *Int. J. Occup. Environ. Med.* **2020**, *11*, 85–94. [[CrossRef](#)]
61. Liao, J.; Yang, F.; Bai, Y.; Yu, W.; Qiao, N.; Han, Q.; Zhang, H.; Guo, J.; Hu, L.; Li, Y.; et al. Metabolomics analysis reveals the effects of copper on mitochondria-mediated apoptosis in kidney of broiler chicken (*Gallus gallus*). *J. Inorg. Biochem.* **2021**, *224*, 111581. [[CrossRef](#)]
62. Zwolak, I. The role of selenium in arsenic and cadmium toxicity: An updated review of scientific literature. *Biol. Trace Elem. Res.* **2020**, *193*, 44–63. [[CrossRef](#)]
63. Hazelhoff, M.H.; Bulacio, R.P.; Torres, A.M. Renal tubular response to titanium dioxide nanoparticles exposure. *Drug Chem. Toxicol.* **2022**, *46*, 1–8. [[CrossRef](#)] [[PubMed](#)]
64. Hajareh Haghighi, F.; Mercurio, M.; Cerra, S.; Salamone, T.A.; Bianymotlagh, R.; Palocci, C.; Romano Spica, V.; Fratoddi, I. Surface modification of TiO₂ nanoparticles with organic molecules and their biological applications. *J. Mater. Chem.* **2023**, *11*, 2334–2366. [[CrossRef](#)]
65. Mbatha, L.S.; Akinyelu, J.; Chukwuma, C.I.; Mokoena, M.P.; Kudanga, T. Current trends and prospects for application of green synthesized metal nanoparticles in cancer and COVID-19 Therapies. *Viruses* **2023**, *15*, 741. [[CrossRef](#)] [[PubMed](#)]
66. Kelany, N.A.; El-Sayed, A.S.A.; Ibrahim, M.A. Aspergillus terreus camptothecin-sodium alginate/titanium dioxide nanoparticles as a novel nanocomposite with enhanced compatibility and anticancer efficiency in vivo. *BMC Biotechnol.* **2023**, *23*, 9. [[CrossRef](#)]
67. Bláhová, L.; Nováková, Z.; Večeřa, Z.; Vrlíková, L.; Dočekal, B.; Dumková, J.; Křůmal, K.; Mikuška, P.; Buchtová, M.; Hampl, A.; et al. The effects of nano-sized PbO on biomarkers of membrane disruption and DNA damage in a sub-chronic inhalation study on mice. *Nanotoxicology* **2020**, *14*, 214–231. [[PubMed](#)]

Disclaimer/Publisher’s Note: The statements, opinions and data contained in all publications are solely those of the individual author(s) and contributor(s) and not of MDPI and/or the editor(s). MDPI and/or the editor(s) disclaim responsibility for any injury to people or property resulting from any ideas, methods, instructions or products referred to in the content.